Math. Res. Lett.
Volume 22, Number 6, 1679–1698, 2015

Asymmetric hyperbolic L-spaces, Heegaard genus, and Dehn filling

Nathan M. Dunfield, Neil R. Hoffman and Joan E. Licata

An L-space is a rational homology 3-sphere with minimal Heegaard Floer homology. We give the first examples of hyperbolic L-spaces with no symmetries. In particular, unlike all previously known L-spaces, these manifolds are not double branched covers of links in S^3. We prove the existence of infinitely many such examples (in several distinct families) using a mix of hyperbolic geometry, Floer theory, and verified computer calculations. Of independent interest is our technique for using interval arithmetic to certify symmetry groups and non-existence of isometries of cusped hyperbolic 3-manifolds. In the process, we give examples of 1-cusped hyperbolic 3-manifolds of Heegaard genus 3 with two distinct lens space fillings. These are the first examples where multiple Dehn fillings drop the Heegaard genus by more than one, which answers a question of Gordon.

1. Introduction

1.1. Asymmetric L-spaces

For a rational homology 3-sphere M, the rank of its Heegaard Floer homology $\widehat{HF}(M)$ is always bounded below by the order of $H_1(M;\mathbb{Z})$, and M is called an *L-space* when this bound is an equality. Lens spaces and other spherical manifolds are all L-spaces, but these are by no means the only examples. In fact, recent work of Boyer, Gordon, and Watson [5] shows that each of the eight 3-dimensional geometries has an L-space. Their work is part of broader efforts to characterize L-spaces via properties not obviously connected to Heegaard Floer theory; specifically, they conjecture that a rational homology sphere is an L-space if and only if its fundamental group is not left-orderable. Although the conjecture has been resolved for seven of the geometries, it remains open for the important case of hyperbolic geometry as well as for most manifolds with non-trivial JSJ decompositions.

All previous examples of hyperbolic L-spaces have come via the following specific type of surgery construction, and one of our main results demonstrates that this is a construction of convenience rather than necessity. A *strong inversion* of a cusped 3-manifold is an orientation preserving, order-two symmetry which acts on each cusp by the elliptic involution; any closed manifold obtained by Dehn filling inherits this symmetry. To date, all hyperbolic L-spaces have been constructed by surgery on strongly invertible manifolds, and moreover, the quotient of the L-space by the induced symmetry was always S^3. Recall that a hyperbolic 3-manifold is *asymmetric* if its only self-isometry is the identity map; by a deep theorem of Gabai, this is equivalent to every self-diffeomorphism being isotopic to the identity [15]. We show the following:

1.2. Theorem. *There exist infinitely many asymmetric hyperbolic L-spaces. In particular, there are hyperbolic L-spaces which are neither regular covers nor regular branched covers of another 3-manifold.*

Among L-spaces which are *not* double branched covers over links in S^3, hyperbolic examples such as those of Theorem 1.2 are the simplest possible in the sense that any such L-space must have a hyperbolic piece in its prime/JSJ decomposition. This is because any graph manifold which is a rational homology sphere, much less an L-space, is a double branched cover over a link in S^3. This was proved by Montesinos in [21, §7.2]; the theorem stated there is paraphrased in the translation below:

1.3. Theorem ([21, §7.2]). *Let M be a graph manifold whose diagram is a tree with each vertex corresponding to a Seifert fibered space over a (punctured) S^2 or (punctured) $\mathbb{R}\mathrm{P}^2$. Then M is a double branched cover of a link L in S^3.*

Note the rational homology sphere assumption implies that the diagram of the graph manifold is a tree. Also, the cases that arise if the tree is a just single vertex are covered in [21, §2-3].

We prove Theorem 1.2 via a combination of hyperbolic geometry, Heegaard Floer theory, and verified computer calculations. The proof of Theorem 1.2 has two parts, the second of which is computer-aided. The first result shows that we need only construct 1-cusped manifolds with certain properties, and the second establishes the existence of such manifolds. Here, the *order* of a lens space is the order of its fundamental group/first homology.

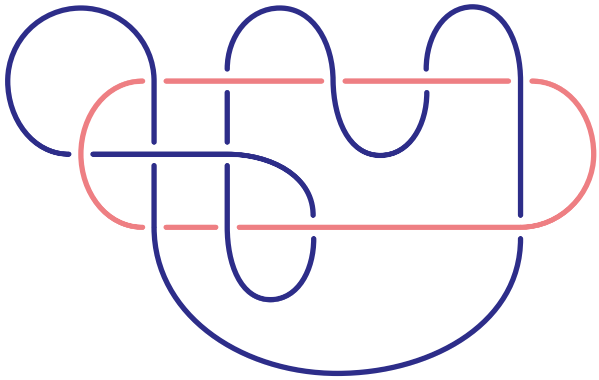

Figure 1.4. The link used in Theorem 4.4 is $L12n1314$ in the Hoste-Thistlewaite census. Our framing conventions for Dehn filling are  and are consistent with SnapPy [10]. Note there is an orientation-preserving homeomorphism of S^3 which interchanges the two components.

2.1. Theorem. *Suppose M is a* 1*-cusped hyperbolic 3-manifold. If M is asymmetric and has two lens space Dehn fillings of coprime order, then there are infinitely many Dehn fillings of M which are asymmetric hyperbolic L-spaces. Moreover, M is the complement of a knot in an integral homology 3-sphere and fibers over the circle with fiber a once-punctured surface.*

4.4. Theorem. *There exist infinitely many 1-cusped hyperbolic 3-manifolds which are asymmetric and have two lens space fillings of coprime order. Specifically, if N is the exterior of the link in Figure 1.4, then for all large $k \in \mathbb{Z}$, the $(6k \pm 1, k)$ Dehn filling on either component of N yields such a manifold.*

In addition to Theorem 4.4, Theorem 4.1 offers a finite number of explicit examples for which the proof is slightly easier. A Heegaard diagram of the simplest of these examples is given in Figure 4.3.

1.5. Heegaard genus, Dehn filling, and the Berge conjecture

Our second main result answers a question of Gordon [16] regarding the existence of manifolds where multiple fillings drop the Heegaard genus by more than one:

1.6. Corollary. *There exist infinitely many 1-cusped hyperbolic 3-manifolds of Heegaard genus three which admit two distinct lens space fillings.*

This corollary follows immediately from Theorem 4.4, as manifolds with genus two Heegaard splittings always have symmetries; the examples of Theorem 4.4 must have Heegaard genus exactly three since the link in Figure 1.4 is 3-bridge.

The interest in L-spaces stems in part from open questions about lens space surgery, with the Berge Conjecture as the chief example. Another interesting feature of Corollary 1.6 is that it provides counterexamples to the following generalization of the Berge Conjecture, since the exterior of any $(1,1)$–knot has Heegaard genus two:

1.7. Conjecture ([1, Conjecture 9]). *If knots $K_1 \subset L(p_1, q_1)$ and $K_2 \subset L(p_2, q_2)$ are longitudinal surgery duals, then up to reindexing, K_2 is a $(1,1)$–knot and $p_2 \geq p_1$.*

We note that these examples do not contradict the Berge Conjecture itself because they are not knot complements in S^3; see the proof of Theorem 4.4 for details.

1.8. Certifying symmetry groups

The hard part of proving Theorems 4.1 and 4.4 is determining the symmetry groups of 23 cusped hyperbolic 3-manifolds, in particular, showing that they are asymmetric. Following Weeks and collaborators [18, 19, 26], we do this by using the Epstein-Penner canonical cellulation; the symmetry group agrees with the combinatorial isomorphisms of this cellulation. For each manifold, we give a rigorous computer-assisted proof that a certain triangulation is the canonical cellulation. We build on the verified computation scheme of [20] for proving the existence of hyperbolic structures. This scheme replaces floating-point computations subject to various kinds of errors with interval arithmetic in order to meet the traditional standards of rigorous proof. Our method for certifying a triangulation as canonical is described in detail in Section 3 and is not specific to the examples here. In addition, the proofs of Theorems 4.1 and 4.4 employ SnapPy [10] to perform combinatorial computations. Both SnapPy and the code for [20] are freely available; the source code and data files used in the computer-assisted proofs in this paper are permanently archived at [12].

As further context for Theorems 4.1 and 4.4, we note that in general it is quite difficult to show a particular 3-manifold is asymmetric. Most proofs that *specific* hyperbolic 3-manifolds are asymmetric hinge on computing a hyperbolic invariant which is not preserved by any possible isometry; see for example the delicate arguments in [24]. One notable exception is the case of complements to certain arborescent knots [4]; since knots are determined by their complements [17], the symmetry group of a knot complement is the same as that of the pair (S^3, K), where additional tools apply. As the referee pointed out to us, the link L in Theorem 4.4 is Montesinos and the symmetry group of (S^3, L) can be computed by [3]. While this is less information than the symmetry group of the exterior of L, it is possible to leverage this fact to a computer-free proof of Theorem 4.4 and hence Theorem 1.2 and Corollary 1.6; see Remark 4.7 for details. However, this alternative approach does not extend to the specific examples in Theorem 4.1 of asymmetric 1-cusped manifolds.

2. Asymmetric L-spaces from cusped manifolds

This section is devoted to the proof of the following result:

2.1. Theorem. *Suppose M is a 1-cusped hyperbolic 3-manifold. If M is asymmetric and has two lens space Dehn fillings of coprime order, then there are infinitely many Dehn fillings of M which are asymmetric hyperbolic L-spaces. Moreover, M is the complement of a knot in an integral homology 3-sphere and fibers over the circle with fiber a once-punctured surface.*

This theorem follows immediately from the next two lemmas, where in the second one we set $N \setminus \partial N \cong M$.

2.2. Lemma. *Suppose M is an asymmetric 1-cusped hyperbolic 3-manifold. Then all but finitely many Dehn fillings of M are hyperbolic and asymmetric.*

2.3. Lemma. *Suppose N is a compact 3-manifold with ∂N a torus. If N has two lens space Dehn fillings of coprime order, then N has infinitely many Dehn fillings which are L-spaces. Moreover, N is the exterior of a knot in an integral homology sphere and fibers over the circle with fiber a surface with one boundary component.*

The proofs of these two lemmas are completely independent and will be familiar to experts in the areas of 3-dimensional hyperbolic geometry and Heegaard Floer theory, respectively.

Proof of Lemma 2.2. Our argument here is motivated by [19], which contains additional details. The key geometric claim is that, for all but finitely many slopes α, the Dehn filled manifold M_α is hyperbolic with the core c of the added solid torus being the *unique* shortest closed geodesic in M_α. Since c is the unique geodesic of its length, any isometry of M_α must send c to itself, setwise if not pointwise. Any isometry of M_α thus induces a self-diffeomorphism of M. Any symmetry of M_α would thus give one of the asymmetric manifold M, and so M_α must also be asymmetric, as desired.

The geometric claim follows from the proof of the Hyperbolic Dehn Surgery Theorem [25, Theorem 5.8.2] as we now explain. Thurston showed that all but finitely many Dehn fillings on M give closed hyperbolic 3-manifolds whose geometry is very close to that of M outside the core curves of the filling solid tori; for further background see [25, §4.6-4.8]. Specifically, for any fixed $\epsilon > 0$, after excluding finitely many slopes α, we can assume that M_α is hyperbolic with the core curve c being a geodesic of length less than ϵ which lives inside a very deep tube whose complement is $(1+\epsilon)$–bi-Lipschitz to a fixed compact subset of M. Taking ϵ much smaller than the length of the shortest closed geodesic in M, it follows that c is the *unique* shortest closed geodesic in M_α. This establishes the geometric claim and hence the lemma. □

Proof of Lemma 2.3. We first show that N is the exterior of a knot in an integral homology sphere. Let α and β be the given slopes where N_α and N_β are lens spaces. Since $H_1(N_\alpha;\mathbb{Z}) = H_1(N;\mathbb{Z})/\langle\alpha\rangle$ and $H_1(N_\beta;\mathbb{Z}) = H_1(N;\mathbb{Z})/\langle\beta\rangle$ are cyclic of coprime order, it follows that $H_1(N;\mathbb{Z})/\langle\alpha,\beta\rangle$ is trivial and hence that $H_1(\partial N;\mathbb{Z}) \to H_1(N;\mathbb{Z})$ is surjective; combining this with “half-lives, half-dies” for $H_1(\partial N;\mathbb{F}_p) \to H_1(N;\mathbb{F}_p)$ for every prime p, it follows that $H_1(N;\mathbb{Z}) \cong \mathbb{Z}$. Let $\mu \in H_1(\partial N;\mathbb{Z})$ be any primitive element whose image generates $H_1(N;\mathbb{Z})$. Then N_μ is an integral homology sphere as desired.

A knot K in a lens space L is *primitive* if $[K]$ generates $H_1(L;\mathbb{Z})$. Since $H_1(\partial N;\mathbb{Z})$ surjects onto $H_1(N;\mathbb{Z})$, it follows that N is the exterior of primitive knots in N_α and N_β; Theorem 6.5 of [2] then implies that N fibers over the circle. An easy consequence of the surjectivity of $H_1(\partial N;\mathbb{Z}) \to H_1(N;\mathbb{Z})$ is that the fiber has only one boundary component.

It remains to show that N has infinitely many L-space fillings, which is a standard consequence of the exact triangle in Heegaard Floer homology, specifically:

2.4. Proposition ([22, Prop 2.1]). *Suppose $\{\eta,\nu\}$ are a basis for $H_1(\partial N;\mathbb{Z})$ and N_η, N_ν, and $N_{\eta+\nu}$ are all rational homology spheres with*

$$|H_1(N_{\eta+\nu};\mathbb{Z})| = |H_1(N_\eta;\mathbb{Z})| + |H_1(N_\nu;\mathbb{Z})|. \tag{2.5}$$

If N_η and N_ν are L-spaces, so is $N_{\eta+\mu}$.

As elements of $H_1(\partial N;\mathbb{Z})$, orient α and β so that the cone $C = \{a\alpha + b\beta \mid a, b \in \mathbb{Z}_{>0}\}$ is disjoint from the kernel of $H_1(\partial N;\mathbb{Z}) \to H_1(N;\mathbb{Z})$. It is enough to show that every primitive lattice point in C corresponds to an L-space filling. Notice first that the homological picture of $(N, \partial N)$ developed above means that the map $C \to \mathbb{N}$ which sends $\gamma \to |H_1(N_\gamma;\mathbb{Z})|$ is the restriction of a linear function. In particular, condition (2.5) will always hold on C. By the Cyclic Surgery Theorem [11], the geometric intersection number $\alpha \cdot \beta$ is 1, and hence we may apply Proposition 2.4 to see that $N_{\alpha+\beta}$ is an L-space. Repeating this argument inductively with the basis $\langle n\alpha + \beta,\ \alpha\rangle$ yields an infinite collection of L-space fillings on N, proving the lemma. One can extend this to all primitive vectors in C with a little more thought, and a complete answer to which N_η are L-spaces is given in [23]. □

3. Certifying canonical triangulations

Triangulations are a basic tool in 3-manifold topology, especially its algorithmic and computational aspects, and the use of ideal triangulations to study hyperbolic structures on 3-manifolds goes back to Thurston [25]. Although every manifold has infinitely many triangulations, a cusped hyperbolic 3-manifold M has a unique *canonical ideal cellulation* which is defined solely in terms of its geometry. Generically —including in all the examples here— this cellulation is an ideal triangulation, called the *canonical triangulation.*

Introduced by Epstein and Penner [13], the canonical cellulation is defined by first embedding the universal cover $\mathbb{H}^3$ of M into $(3+1)$-dimensional Minkowski space. Choose disjoint horotorus neighborhoods of each cusp in M which all have the same volume. Upstairs in $\mathbb{H}^3$, these neighborhoods lift to a $\pi_1(M)$–invariant packing of horoballs. In the Minkowski model, each horoball B has a corresponding lightcone vector v_B, where $B = \left\{ w \in \mathbb{H}^3 \;\middle|\; v_B \cdot w \leq -1 \right\}$. The convex hull of the lightcone vectors associated to the set of cusps has a natural cellulation of its boundary, and projecting this radially defines a cellulation of $\mathbb{H}^3$. Since this cellulation is preserved both by the action of $\pi_1(M)$ and also by the lifts of isometries of M, it descends to a cellulation of M which is preserved by its isometry group; in particular, we get the following key tool:

3.1. Corollary ([18]). *The elements of the isometry group of M correspond precisely to the combinatorial isomorphisms of its canonical cellulation. In* *particular, if the canonical cellulation has no nontrivial combinatorial isomorphisms, then M is asymmetric.*

From now on, let $\mathcal{T}$ denote an ideal triangulation of M where each topological tetrahedron has been assigned a shape: an isometry type of an ideal tetrahedron with geodesic sides in $\mathbb{H}^3$. Each shape is specified by a complex number, and these numbers must satisfy certain polynomial conditions which ensure that these geometric tetrahedra glue up to give the complete hyperbolic structure on M [25, 27].

In [26], Weeks gave an easy way to check whether such a given geometric ideal triangulation is canonical. Let X be one of the ideal tetrahedra, and label its vertices $\{0, 1, 2, 3\}$. For some fixed horotorus cross section of the cusp near vertex i, let R_i^X denote the circumradius of the cross section and let θ_{ij}^X denote the dihedral angle of the edge from vertex i to vertex j. For the face F of X opposite vertex i, define

$$\mathrm{Tilt}(X, F) = R_i^X - \sum_{k \neq i} R_k^X \cos \theta_{ik}^X \tag{3.2}$$

If Y is the other tetrahedron sharing F as a face, set $\mathrm{Tilt}(F) := \mathrm{Tilt}(X, F) + \mathrm{Tilt}(Y, F)$. With this notation, Weeks' criterion is as follows:

3.3. Theorem ([26, Prop 3.1, Thm 5.1]). *A geometric ideal triangulation $\mathcal{T}$ of a cusped manifold M is its canonical cellulation if and only if every face F of $\mathcal{T}$ has* $\mathrm{Tilt}(F) < 0$.

Geometrically, the gluing at the face F is convex, flat, or concave, depending on whether $\mathrm{Tilt}(F)$ is negative, zero, or positive.

3.4. Finding the canonical triangulation

We next explain how SnapPy attempts to find the canonical cellulation. This gives context for our results and highlights the necessity of a verified computation by showing what could go wrong. However, the reader interested only in the proofs of our results can safely skip ahead to §3.5.

In [26], Weeks gave a procedure, implemented in [10], to transform an arbitrary geometric triangulation $\mathcal{T}$ of a hyperbolic 3-manifold M into the canonical cellulation. Neglecting for the moment the numerical issues inherent in floating-point arithmetic, his procedure is the following:

(1) If $\mathrm{Tilt}(F) < 0$ for every face of $\mathcal{T}$, then $\mathcal{T}$ itself is the canonical triangulation by Theorem 3.3. If $\mathrm{Tilt}(F) \leq 0$ for every face, then $\mathcal{T}$ is

a tetrahedral subdivision of the canonical cellulation. In either case, the procedure terminates.

(2) If there is a face F with $\mathrm{Tilt}(F) > 0$ and with the property that performing a 2-to-3 Pachner move on F creates only positively oriented tetrahedra, then replace $\mathcal{T}$ with the result of this 2-to-3 move and go back to Step 1.

(3) If there is a valence three edge E of $\mathcal{T}$ with a face F incident to E having $\mathrm{Tilt}(F) \geq 0$, then replace $\mathcal{T}$ with the result of the 3-to-2 Pachner move on E and go back to Step 1.

(4) If some face F has $\mathrm{Tilt}(F) > 0$ but no moves permitted in Steps 2 and 3 are possible, do a sequence of random Pachner moves to replace $\mathcal{T}$ with a different geometric triangulation and return to Step 1.

While in practice this procedure almost always succeeds in finding the canonical cellulation, it is not known to terminate with probability 1. More significantly for us, even when it does terminate, floating-point issues may cause the cellulation returned *not* to be canonical. Specifically, as the shapes are known only approximately and round-off errors may accumulate, SnapPy may conclude erroneously that $\mathrm{Tilt}(F) \leq 0$ for all F. This is not merely a theoretical concern. For example, there is a certain 16 tetrahedra triangulation of the exterior to the link $L10a154$ (included in [12]) where SnapPy identifies the wrong cellulation as canonical; in this case, the actual canonical cellulation has non-tetrahedral cells, which is the hardest case because some tilts are zero.

3.5. Certifying hyperbolic structures

Before rigorously finding the canonical triangulation, we must first certify the existence of a hyperbolic structure. For this we used the verification scheme of [20] which replaces floating-point computations with rigorous interval arithmetic. In interval arithmetic, a number $z \in \mathbb{C}$ is partially specified by giving a rectangle with vertices in $\mathbb{Q}(i)$ which contains z. Because the vertices are rational, such intervals can be exactly stored on a computer and rigorously combined by the operations $+, -, \cdot, /$ to create other such intervals. The cost is that the sizes of the rectangles grow with the number of operations. Given an ideal triangulation $\mathcal{T}$ of a 3-manifold M, in favorable circumstances the verification scheme of [20] produces an interval for each tetrahedral shape, together with a proof that the actual hyperbolic structure has shapes lying in those intervals.

3.6. Certifying canonical triangulations

We now explain how to extend the work of [20] to rigorously certify a triangulation $\mathcal{T}$ of M as canonical. The basic idea is to use interval arithmetic when checking the hypotheses of Theorem 3.3, starting from the guaranteed shape intervals produced by [20]. Note that for a real interval r, it makes sense to say that say $r < 0$ when both of the endpoints of r are negative. (In contrast, there is no notion of equality for intervals since an interval is just a stand-in for some unknown number inside it.) Thus if we compute $\mathrm{Tilt}(F)$ as a real interval from the guaranteed shape intervals, we can potentially certify that $\mathrm{Tilt}(F) < 0$ as required by Theorem 3.3. From (3.2), one sees that it suffices to compute the quantities R_i^X and $\cos\left(\theta_{i,j}^X\right)$.

We begin with the easier case where M has a single cusp. We construct a particular cusp cross section by first choosing a corner of a fixed tetrahedron and then selecting a horospherical Euclidean triangle whose first side has length 1. The (known) shape of the tetrahedron determines the other two sides of this cusp triangle, and from there, one can propagate the cusp cross section to adjacent tetrahedra. Since there is only one cusp, this initial choice determines the whole cross section. The resulting "cusp cross section" could be too large to be embedded, but it represents an actual cross section up to a uniform dilation; since (3.2) is homogenous in the R_i^X, this has no effect on checking the hypotheses of Theorem 3.3.

The quantity R_i^X is the circumradius of the corresponding cusp triangle, and the circumradius of a triangle may be computed from the lengths of its edges using only the operations $+, -, \cdot, /$ and $\sqrt{}$, all of which are supported by the interval arithmetic scheme of [20]; see §3.1 of that paper for details. The cosines of the dihedral angles that appear in (3.2) can be similarly computed; if the (i, j) edge has shape $z = a + bi$, we have $\cos\left(\theta_{i,j}^X\right) = \cos\left(\arg(z)\right) = a/\sqrt{a^2 + b^2}$.

Thus in the 1-cusped case, we can compute tilt intervals from the initial shape intervals and hence potentially apply Theorem 3.3 in a rigorous way; we will do precisely this for the 22 manifolds of Theorem 4.1.

3.7. Multiple cusps

When M has multiple cusps, as in the proof of Theorem 4.4, there is an additional subtlety. Specifically, the canonical cellulation is defined in terms of cusp cross sections which *all have the same area*. As mentioned above, interval arithmetic does not support the notion of equality. In order to describe our solution to this issue, we must first introduce some more precise notation. Letting $[a]$ and $[b]$ denote intervals, we say that $[a] < [b]$ if $a < b$ for all $a \in [a]$ and $b \in [b]$. We extend this notation, using $[C]$ to denote a cusp cross section which is computed by interval arithmetic from the guaranteed shape data as in §3.6, and we say that an actual cusp cross section C lies in $[C]$ if all its Euclidean triangles have side lengths in the corresponding interval side lengths of $[C]$. In particular, if C is in $[C]$, then $\mathrm{Area}(C)$ is in $\mathrm{Area}([C])$, where the latter is an honest interval.

For notational simplicity, let us start with the case where M has two cusps. Let $[C_0]$ and $[C_1]$ be cusp cross sections constructed from the shape data as above. Scale $[C_1]$ to create $[C_1^-]$ and $[C_1^+]$ where the following holds in the interval sense:

$$\mathrm{Area}\left([C_1^-]\right) < \mathrm{Area}\left([C_0]\right) < \mathrm{Area}\left([C_1^+]\right) \tag{3.8}$$

If F is a face of $\mathcal{T}$, we use $\mathrm{Tilt}(F, [C_0], [C_1])$ to denote the tilt interval of F with respect to the cusps $[C_0]$ and $[C_1]$ computed as in §3.6. The proof of Theorem 4.4 rests on the following:

3.9. Proposition. *Suppose $\mathcal{T}$ is a geometric triangulation of a 2-cusped manifold M with guaranteed shape intervals, and suppose further that $[C_0]$, $[C_1^-]$, and $[C_1^+]$ are cusp cross sections satisfying (3.8). If for every face F of $\mathcal{T}$ we have $\mathrm{Tilt}\big(F, [C_0], [C_1^-]\big) < 0$ and $\mathrm{Tilt}\big(F, [C_0], [C_1^+]\big) < 0$, then $\mathcal{T}$ is the canonical triangulation of M.*

Proof. Fix actual cusp cross sections C_0, C_1^+, C_1^- in $[C_0], [C_1^-], [C_1^+]$, respectively. The hypotheses imply $\mathrm{Area}(C_1^-) < \mathrm{Area}(C_0) < \mathrm{Area}(C_1^+)$. Let C_1' be an actual cross section for the second cusp with $\mathrm{Area}(C_1') = \mathrm{Area}(C_0)$. Thinking of cusp cross sections as vectors whose coordinates are the circumradii of their constituent Euclidean triangles, we can view C_1' as a convex combination

$$C_1' = (1-t) \cdot C_1^- + t \cdot C_1^+ \quad \text{for some } t \in (0,1).$$

For any face F, the function $\mathrm{Tilt}(F, C_0, \,\cdot\,)$ is linear in the remaining input, and so since both $\mathrm{Tilt}\big(F, C_0, C_1^-\big)$ and $\mathrm{Tilt}\big(F, C_0, C_1^+\big)$ are negative by our hypotheses, we must have $\mathrm{Tilt}(F, C_0, C_1') < 0$. In particular, since $\mathrm{Area}(C_0) = \mathrm{Area}(C_1')$, Theorem 3.3 now implies that $\mathcal{T}$ is canonical. □

Proposition 3.9 extends easily to manifolds with three or more cusps. First fix some $[C_0]$ for the first cusp, and then for each further cusp, choose a pair of cross sections $[C_n^{\pm}]$ with

$$\text{Area}\left([C_n^-]\right) < \text{Area}\left([C_0]\right) < \text{Area}\left([C_n^+]\right).$$

If for every face F and every pattern of signs $\{\epsilon_n\}$ one has

$$\text{Tilt}([C_0], [C_1^{\epsilon_1}], [C_2^{\epsilon_2}], \ldots, [C_m^{\epsilon_m}]) < 0,$$

then $\mathcal{T}$ must be canonical. The point is again that the actual equal area cross sections are convex combinations of cross sections in the $[C_n^{\pm}]$, all of which have negative tilts when combined with $[C_0]$.

3.10. Remark. The subsequent paper [14] gives an elegant simplification of our technique in the multicusped case (see their Section 3.4) and they provide an implementation of their approach which works for any number of cusps.

3.11. Canonical cellulations with more complicated cells

Canonical cellulations are generically triangulations, but it would be useful to be able to certify canonicity of cellulations with more complicated cells, especially as these include some of the most symmetric examples. It is unclear whether this can be done directly in the context of interval arithmetic, since the lack of equality testing means we can not be sure that some tilt is precisely zero, exactly the condition that leads to non-tetrahedral cells. In small cases, one should be able to use exact arithmetic in a number field to deal with this, as in [9], but the interval arithmetic techniques of [20] can be successfully applied to *much* more complicated manifolds.

4. Asymmetric manifolds with lens space fillings

Before proving Theorem 4.4, we warm up with the following easier and more concrete result, which, when combined with Theorem 2.1, also suffices to prove Theorem 1.2.

4.1. Theorem. *Table 4.2 lists 22 distinct 1-cusped hyperbolic 3-manifolds which are asymmetric and have two lens space fillings of coprime order.*

We provide a rigorous computer-assisted proof of Theorem 4.1 using SnapPy [10], the verification scheme of [20], and the techniques given in Section 3. These examples were found in the census of 1-cusped hyperbolic 3-manifolds

M	#tets	$M_{(1,0)}$	$M_{(0,1)}$	g	vol(M)	systole
$v3372^*$	7	$L(7,1)$	$L(19,7)$	10	6.541194	0.952884
$t10397$	8	$L(11,2)$	$L(14,3)$	12	6.880362	0.911798
$t10448$	8	$L(17,5)$	$L(29,8)$	15	6.891314	0.716411
$t11289^*$	8	$L(11,2)$	$L(26,7)$	15	7.084874	0.576033
$t11581$	8	$L(7,1)$	$L(31,12)$	16	7.180413	0.767839
$t11780$	8	$L(23,7)$	$L(6,1)$	12	7.232671	0.643558
$t11824$	8	$L(34,13)$	$L(19,4)$	19	7.246332	0.480409
$t12685$	8	$L(14,3)$	$L(29,8)$	18	7.674889	0.693829
$o9^*_{34328}$	10	$L(13,2)$	$L(34,13)$	19	7.529794	0.312418
$o9_{35609}$	10	$L(50,19)$	$L(29,8)$	27	7.631975	0.237482
$o9^*_{35746}$	10	$L(17,3)$	$L(41,12)$	24	7.642118	0.238001
$o9_{36591}$	9	$L(55,21)$	$L(31,7)$	31	7.707673	0.188586
$o9_{37290}$	9	$L(31,12)$	$L(19,4)$	22	7.762770	0.442218
$o9_{37552}$	9	$L(35,8)$	$L(13,3)$	18	7.781895	0.408545
$o9_{38147}$	9	$L(29,12)$	$L(41,11)$	27	7.831770	0.392648
$o9_{38375}$	9	$L(17,3)$	$L(29,8)$	24	7.851404	0.349858
$o9_{38845}$	9	$L(13,2)$	$L(18,5)$	15	7.896384	0.770335
$o9_{39220}$	10	$L(13,2)$	$L(46,17)$	28	7.930877	0.304931
$o9_{41039}$	10	$L(13,2)$	$L(21,8)$	16	8.122543	0.916284
$o9_{41063}$	9	$L(26,7)$	$L(41,11)$	30	8.126169	0.386869
$o9_{41329}$	9	$L(34,9)$	$L(49,18)$	34	8.159350	0.364220
$o9_{43248}$	10	$L(37,8)$	$L(18,5)$	23	8.444914	0.689245

Table 4.2. The 22 manifolds of Theorem 4.1. Here, "#tets" refers to the canonical triangulation supplied in [12] and g is the genus of the fibration of M over the circle (whose existence follows from Theorem 2.1) computed via the Alexander polynomial. The lens spaces were identified using Regina [7]. The manifolds marked with a $*$ also appear in Theorem 4.4. The data is all rigorous with the exception of the volume and systole columns, which were approximated numerically, as the methods of [20] have not yet been extended to those quantities. Note that none of these manifolds are knot complements in S^3, since the pair of lens space surgeries have fundamental groups whose orders differ by more than one.

with at most 9 tetrahedra [6, 8] by a brute-force search through these 59,107 manifolds.

Proof of Theorem 4.1. The 22 manifolds are specified by particular triangulations that are included in [12]. For each triangulation $\mathcal{T}$, we proved the following:

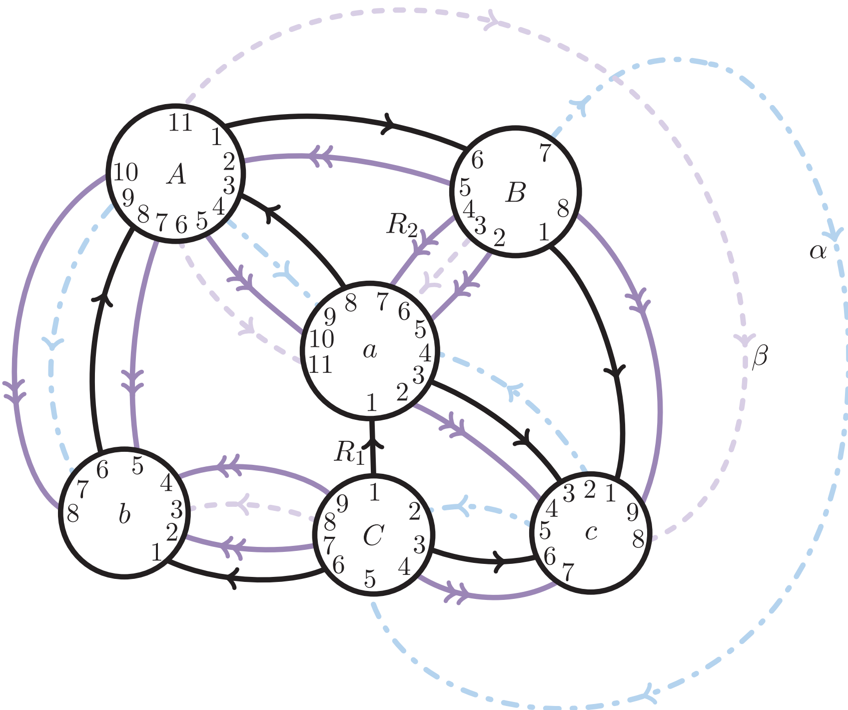

Figure 4.3. A Heegaard diagram for the first manifold $v3372$ in Table 4.2, corresponding to $\langle a, b, c \mid R_1 := ab^{-1}a^{-2}c^2bc = 1,\ \ R_2 := aba^{-1}c^2ba^2bcb = 1\rangle$. Also shown are the slopes $\alpha = c^{-2}a^2b$ and $\beta = cba^2$ which give lens spaces $L(7,1)$ and $L(19,7)$, oriented so any positive combination of them gives an L-space.

(a) *The manifold M underlying $\mathcal{T}$ is hyperbolic.*

We used [20] to find intervals which are guaranteed to contain shapes for the tetrahedra of $\mathcal{T}$ which give rise to an actual complete hyperbolic structure on M.

(b) *The triangulation $\mathcal{T}$ is the canonical cellulation of M.*

Doing arithmetic with the interval shapes as described in §3.6, we verified that all the inequalities in Theorem 3.3 hold, and hence $\mathcal{T}$ is canonical.

(c) *M is asymmetric.*

We used SnapPy to find all combinatorial self-isomorphisms of $\mathcal{T}$; as there was only the identity, asymmetry follows from Corollary 3.1.

(d) *M has two lens space fillings of coprime order.*
We used SnapPy to check that the $(1, 0)$ and $(0, 1)$ Dehn fillings on M (with respect to the cusp framing specified in the triangulation file for $\mathcal{T}$) have fundamental groups with presentations that are obviously those of finite cyclic groups of coprime order; the Geometrization Theorem implies that these are lens spaces. This combinatorial step is also performed rigorously by SnapPy. (Regina [7] can go further and identify the particular lens spaces directly, without appealing to geometrization; this data is included in Table 4.2.)

To finish off Theorem 4.1, it remained to show that the examples are distinct. For this, we checked that no two of the triangulations were combinatorially isomorphic. By (b), this implies the 22 manifolds are not isometric and hence not homeomorphic. Alternatively, this is proved in [6] by different methods.

Complete source code for this proof is available at [12]. As a precaution, two disjoint subsets of the authors wrote independent implementations of step (b), and the entire proof was executed from a single script. Additionally, our code is robust enough to run on all 59,107 one-cusped census manifolds in [6]; excluding the 64 cases where SnapPy believes there are canonical cells which are not tetrahedra, we were able to certify the canonical triangulations for all of these manifolds. □

We next extend the phenomena exhibited in Theorem 4.1 to an infinite family of examples; note that our conventions for Dehn filling are specified in Figure 1.4.

4.4. Theorem. *There exist infinitely many 1-cusped hyperbolic 3-manifolds which are asymmetric and have two lens space fillings of coprime order. Specifically, if N is the exterior of the link in Figure 1.4, then for all large $k \in \mathbb{Z}$, the $(6k \pm 1, k)$ Dehn filling on either component of N yields such a manifold.*

Proof. Let N_k denote the $(6k + 1, k)$ Dehn filling on the second cusp of N; we focus on this case first for notational simplicity, leaving the $(6k - 1, k)$ Dehn filling for later. The theorem in this case follows immediately from the next two lemmas.

4.5. Lemma. *For all $k \in \mathbb{Z}$ with $|k|$ sufficiently large, the manifold N_k is hyperbolic and asymmetric.*

4.6. Lemma. *For all $k \in \mathbb{Z}$, the $(1,0)$ and $(4,1)$ Dehn fillings on the remaining cusp of N_k are lens spaces of coprime orders $|6k+1|$ and $|15k+4|$, respectively.*

Proof of Lemma 4.5. Let $\mathcal{T}$ be the particular triangulation of N included in [12]. Using [20] and Proposition 3.9, we verified that $\mathcal{T}$ is in fact the canonical triangulation of N. The triangulation $\mathcal{T}$ has only two combinatorial isomorphisms: the identity and one that interchanges the two cusps. Hence by Corollary 3.1 the only isometry of N that preserves the each cusp is the identity. The lemma now follows from the argument used to prove Lemma 2.2. □

4.7. Remark. The referee kindly pointed out that the link L in Figure 1.4 is the Montesinos link $M(0;(5,3),(3,-2),(5,1))$, and hence its symmetry group $\pi_0\big(\mathrm{Diff}(S^3,L)\big)$ can be computed using Boileau and Zimmermann [3]. Unlike the case of knots [17], a symmetry of a link exterior need not send meridians to meridians; for example, the symmetry group of the $(-2,3,8)$-pretzel link is $\mathbb{Z}/2\mathbb{Z}$, but the symmetry group of its exterior has order 8. While the proof of Lemma 4.5 given above requires that we know the full symmetry group of the exterior N, rather than just $\pi_0\big(\mathrm{Diff}(S^3,L)\big)$, by working harder one can prove Lemma 4.5 from the results in [3] without reference to a canonical triangulation of N. We now sketch this alternative argument.

Using [3], one computes that the symmetry group of the link L is $\mathbb{Z}/2\mathbb{Z}$ where the generator interchanges the two components. If infinitely many N_k admit a nontrivial symmetry, then since the symmetry group of N is finite, there is an infinite set of indices k_i where said symmetry of N_{k_i} is induced by a fixed symmetry f of N. We will show that f is a symmetry of the underlying link L and consequently f must be the identity. Let C_1 and C_2 be torus cross-sections for the two cusps of N. For each i, the symmetry f preserves the unoriented isotopy class of the Dehn filling curve $\gamma_i \subset C_2$ used to form N_{k_i}. Again passing to a subsequence, we can assume that f either preserves the *oriented* isotopy class of all γ_i or reverses the orientation on all of them. In the former case, it follows that f restricted to C_2 is isotopic to the identity; in the latter, it must be isotopic to the elliptic involution. Since the two components of L have nonzero linking number, the maps $H_1(C_i;\mathbb{Z}) \to H_1(N;\mathbb{Z})$ are both injective; it follows that the action of f on C_2 determines the action of f on $H_1(C_1;\mathbb{Z})$. Consequently, in either case, the map f must preserve the unoriented isotopy classes of the meridians which record L in both C_1 and C_2, and hence comes from a symmetry of (S^3, L) as claimed.

Proof of Lemma 4.6. It is clear from Figure 1.4 that both link components are unknotted; the $(1, 0)$ filling on N_k is thus a lens space of order $|6k + 1|$.

Turning now to the other filling, let P denote the $(4, 1)$ filling of the first cusp of N. The key idea is that P is Seifert fibered over the disc with two exceptional fibers of orders 3 and 5, and hence has infinitely many lens space Dehn fillings; we chose the fillings defining the N_k to be these lens space slopes. If $\langle \mu, \lambda \rangle$ is a meridian-longitude basis (with respect to the standard link framing) for $\pi_1(\partial P)$, SnapPy easily computes that

$$\pi_1(P) = \left\langle a, b \;\middle|\; b^3 a^5 = 1 \right\rangle \quad \text{with } \mu = b^2 a^2 \text{ and } \beta := \mu^6 \lambda = b^3 = a^{-5}.$$

In particular, the $(6k + 1, k)$ filling, which is along the slope $\mu\beta^k$, has fundamental group $\left\langle a, b \;\middle|\; b^3 a^5 = 1,\ \mu\beta^k = b^2 a^{2-5k} = 1 \right\rangle$. Replacing the second relator by its product on the left with the inverse of the first relator yields the following presentation:

$$\left\langle a, b \;\middle|\; b^3 a^5 = 1,\ a^{-(5k+3)} = b \right\rangle \ = \ \left\langle a \;\middle|\; a^{15k+4} = 1 \right\rangle$$

Thus the $(4, 1)$ filling on N_k is a lens space whose first homology has order $|15k + 4|$. We conclude the proof for the $(6k + 1, k)$ filling by noting that $p_1 = 6k + 1$ and $p_2 = 15k + 4$ are coprime, since $-(5k + 3)p_1 + (2k + 1)p_2 = 1$ for any k. □

The $(6k - 1, k)$ case differs only in that the lens spaces have order $p_1' = 6k - 1$ and $|p_2'|$, where $p_2' = 15k - 4$. These are coprime since $-(5k - 3)p_1' + (2k - 1)p_2' = 1$. □

Acknowledgements

The authors gratefully thank Ken Baker, Francis Bonahon, Craig Hodgson, Adam Levine, and Jessica Purcell for many helpful conversations. Dunfield was partially supported by US NSF grant #DMS-1106476 and a Simons Fellowship; this work was partially done while he was visiting the University of Melbourne. Hoffman was supported by the ARC Grant DP130103694 and thanks the Mathematical Sciences Institute at the Australian National University for hosting him during part of this work. We also thank the referee for their very helpful comments, especially for pointing us to the work of [3] which is discussed in Remark 4.7.

References

[1] K. L. Baker, B. G. Doleshal and N. Hoffman, *On manifolds with multiple lens space filings* (2013). To appear in Boletín de la Sociedad Matemática Mexicana.

[2] M. Boileau, S. Boyer, R. Cebanu and G. S. Walsh, *Knot commensurability and the Berge conjecture*. Geom. Topol., **16** (2012), no. 2, 625–664.

[3] M. Boileau and B. Zimmermann, *Symmetries of nonelliptic Montesinos links*. Math. Ann., **277** (1987), no. 3, 563–584.

[4] F. Bonahon and L. Siebenmann, *New geometric splittings of classical knots, and the classification and symmetries of arborescent knots* (2010).

[5] S. Boyer, C. M. Gordon and L. Watson, *On L-spaces and left-orderable fundamental groups*. Math. Ann., **356** (2013), no. 4, 1213–1245.

[6] B. A. Burton, *The cusped hyperbolic census is complete*. Preprint 2014, 32 pages.

[7] B. A. Burton, R. Budney, W. Pettersson, et al., *Regina 4.95: Software for 3-manifold topology and normal surface theory*. Available from `http://regina.sourceforge.net/`, 1999–2014.

[8] P. J. Callahan, M. V. Hildebrand and J. R. Weeks, *A census of cusped hyperbolic* 3*-manifolds*. Math. Comp., **68** (1999), no. 225, 321–332. With microfiche supplement.

[9] D. Coulson, O. A. Goodman, C. D. Hodgson and W. D. Neumann, *Computing arithmetic invariants of 3-manifolds*. Experiment. Math., **9** (2000), no. 1, 127–152.

[10] M. Culler, N. M. Dunfield and J. R. Weeks, *SnapPy v2.2, a computer program for studying the geometry and topology of 3-manifolds*. Available from `http://snappy.computop.org`, (2014/7/8).

[11] M. Culler, C. M. Gordon, J. Luecke and P. B. Shalen, *Dehn surgery on knots*. Ann. of Math. (2), **125** (1987), no. 2, 237–300.

[12] N. M. Dunfield, N. R. Hoffman and J. E. Licata, *Ancillary files with the arXiv version of this paper*.

[13] D. B. A. Epstein and R. C. Penner, *Euclidean decompositions of noncompact hyperbolic manifolds*. J. Differential Geom., **27** (1988), no. 1, 67–80.

[14] E. Fominykh, S. Garoufalidis, M. Goerner, V. Tarkaev and A. Vesnin, *A census of tetrahedral hyperbolic manifolds.* Preprint 2015, 26 pages.

[15] D. Gabai, *The Smale conjecture for hyperbolic 3-manifolds:* $\mathrm{Isom}(M^3) \simeq \mathrm{Diff}(M^3)$. J. Differential Geom., **58** (2001), no. 1, 113–149.

[16] C. M. Gordon, *Lecture at AIM Workshop on Triangulations, Heegaard Splittings, and Hyperbolic Geometry.* December, 2007.

[17] C. M. Gordon and J. Luecke, *Knots are determined by their complements.* J. Amer. Math. Soc., **2** (1989), no. 2, 371–415.

[18] S. R. Henry and J. R. Weeks, *Symmetry groups of hyperbolic knots and links.* J. Knot Theory Ramifications, **1** (1992), no. 2, 185–201.

[19] C. D. Hodgson and J. R. Weeks, *Symmetries, isometries and length spectra of closed hyperbolic three-manifolds.* Experiment. Math., **3** (1994), no. 4, 261–274.

[20] N. Hoffman, K. Ichihara, M. Kashiwagi, H. Masai, S. Oishi and A. Takayasu, *Verified computations for hyperbolic 3-manifolds* (2013). Code available from: `http://www.oishi.info.waseda.ac.jp/~takayasu/hikmot/`.

[21] J. M. Montesinos, *Variedades de seifert que son recubricadores ciclicos rami cados de dos hojas, Boletino Soc.* Mat. Mexicana, **18** (1973) 1–32.

[22] P. Ozsváth and Z. Szabó, *On knot Floer homology and lens space surgeries.* Topology, **44** (2005), no. 6, 1281–1300.

[23] J. Rasmussen, *Lens space surgeries and L-space homology spheres.* Preprint 2007, 23 pages.

[24] R. Riley, *Parabolic representations and symmetries of the knot 932, from:\ Computers and Geometry and Topology",(MC Tangora, editor).* Lecture Notes in Pure and Applied Math., **114** 297–313.

[25] W. P. Thurston, *The geometry and topology of 3-manifolds* (1978–80, 2002). Lecture notes, 360 pages.

[26] J. R. Weeks, *Convex hulls and isometries of cusped hyperbolic* 3-*manifolds.* Topology Appl., **52** (1993), no. 2, 127–149.

[27] J. R. Weeks, *Computation of hyperbolic structures in knot theory.* In: Handbook of knot theory, 461–480, Elsevier B. V., Amsterdam (2005).

Dept. of Math., MC-382, University of Illinois
1409 W. Green St., Urbana, IL 61801, USA
E-mail address: nathan@dunfield.info

School of Math. and Stat., University of Melbourne
Parkville, VIC 3010, Australia
E-mail address: nhoffman@ms.unimelb.edu.au

Mathematical Sciences Institute, John Dedman Bldg 27
The Australian National University 0200, Australia
E-mail address: joan.licata@anu.edu.au

Received April 14, 2015